Final version published as: Macauley, M. S., & Vocadlo, D. J. (2009). Enzymatic characterization and inhibition of the nuclear variant of human O-GlcNAcase. Carbohydrate Research, 344(9), 1079–1084. https://doi.org/10.1016/j.carres.2009.04.017.

Enzymatic characterization and inhibition of the nuclear variant of human *O*-GlcNAcase

Matthew S. Macauley, David J. Vocadlo *

Department of Chemistry, Simon Fraser University, 8888 University Drive, Burnaby, British Columbia, Canada V5A 1S6

ARTICLE INFO

Article history:
Received 14 February 2009
Received in revised form 15 April 2009
Accepted 15 April 2009
Available online 20 April 2009

Keywords:
O-GlcNAcase
OGA isoform
MGEA5
Nuclear variant
β-*N*-Acetylglucosaminidase
O-GlcNAc

ABSTRACT

Increasing cellular *O*-GlcNAc levels through pharmacological inhibition of *O*-GlcNAcase, the enzyme responsible for removal of the *O*-GlcNAc post-translational modification, is being increasingly used to aid in discerning the roles played by this form of intracellular glycosylation. Interestingly, two forms of *O*-GlcNAcase have been studied; a full-length isoform that is better characterized, and a shorter nuclear-localized variant, arising from failure to splice out one intron, which has not been as well characterized. Given the increasing use of *O*-GlcNAcase inhibitors as research tools, we felt that a clear understanding of how these inhibitors affect both isoforms of *O*-GlcNAcase is important for proper interpretation of studies making use of these inhibitors in cell culture and in vivo. Here we describe an enzymatic characterization of the nuclear variant of human *O*-GlcNAcase. We find that this short nuclear variant of *O*-GlcNAcase, which has the identical catalytic domain as the full-length enzyme, has similar trends in a pH-rate profile and Taft linear free energy analysis as the full-length enzyme. These findings strongly suggest that both enzymes use broadly similar transition states. Consistent with this interpretation, the short isoform is potently inhibited by several previously described inhibitors of full-length *O*-GlcNAcase including PUGNAc, NAG-thiazoline, and the selective *O*-GlcNAcase inhibitor NButGT. These findings contrast with earlier studies and suggest that studies using *O*-GlcNAcase inhibitors in cultured cells or in vivo can be interpreted with the knowledge that both these forms of *O*-GlcNAcase are inhibited when present.

1. Introduction

Within higher eukaryotes, numerous nucleocytoplasmic proteins are post-translationally modified with *N*-acetylglucosamine (GlcNAc) residues O-linked to certain serine or threonine residues (*O*-GlcNAc).[1,2] Unlike glycosylation occurring within the secretory pathway, *O*-GlcNAc is a dynamic modification similar in some ways to phosphorylation; the modification can be cleaved off and reinstalled from the polypeptide backbone more quickly then the protein is turned over.[3,4] Two enzymes are involved in regulating the dynamic cycling of *O*-GlcNAc. *O*-GlcNAc transferase (OGT)[5] installs *O*-GlcNAc at appropriate serine or threonine residues of target proteins, whereas *O*-GlcNAcase (OGA)[6] acts to remove the modification and returns residues to their unmodified state. The catalytic mechanism of FL-OGA has been shown to proceed in two steps, via an oxazoline intermediate, to yield the β-anomer of the free GlcNAc hemiacetal.[7] This catalytic mechanism, and formation of the oxazoline intermediate, relies on the involvement of the 2-acetamido group of the substrate (Fig. 1a). In the first step of the reaction, this group acts as a nucleophile to attack the anomeric center and displace the leaving group. One enzymic carboxylate (Asp174) likely acts as a general base to enhance nucleophilicity of the acetamido group while another enzymic carboxylic acid (Asp175) acts as a general acid catalyst to facilitate departure of the leaving group.[8,9] The second step of the reaction is the near microscopic reverse of the first step; attack of water at the anomeric center is facilitated by an enzymic base (Asp175) and the acetamido group is expelled from the anomeric center with Asp174 likely acting as a general acid. How these catalytic activities of OGT and OGA are regulated within cells is slowly emerging[10,11] and shorter isoforms of both enzymes that stem from alternative splicing have been described.[12–14] Although these shorter isoforms have only been partially characterized, they have been reported to have altered properties such as catalytic activity, substrate specificity, and cellular localization.[14–17]

The gene encoding *O*-GlcNAcase (*MGEA5*) was shown by Comptesse et al. to undergo alternative splicing to generate a truncated protein.[14] When intron 10 fails to be spliced out, a transcript is generated that encodes a protein having a 662 amino acid N-terminal section identical to the full-length protein (OGA-FL) and an additional 15 amino acid C-terminal piece arising from the start of intron 10 (Fig. 1b). Such a protein (OGA-NV) therefore lacks the C-terminal domain of OGA. This C-terminal domain has been

* Corresponding author. Tel.: +1 778 782 3530; fax: +1 778 782 3765.
E-mail address: dvocadlo@sfu.ca (D.J. Vocadlo).

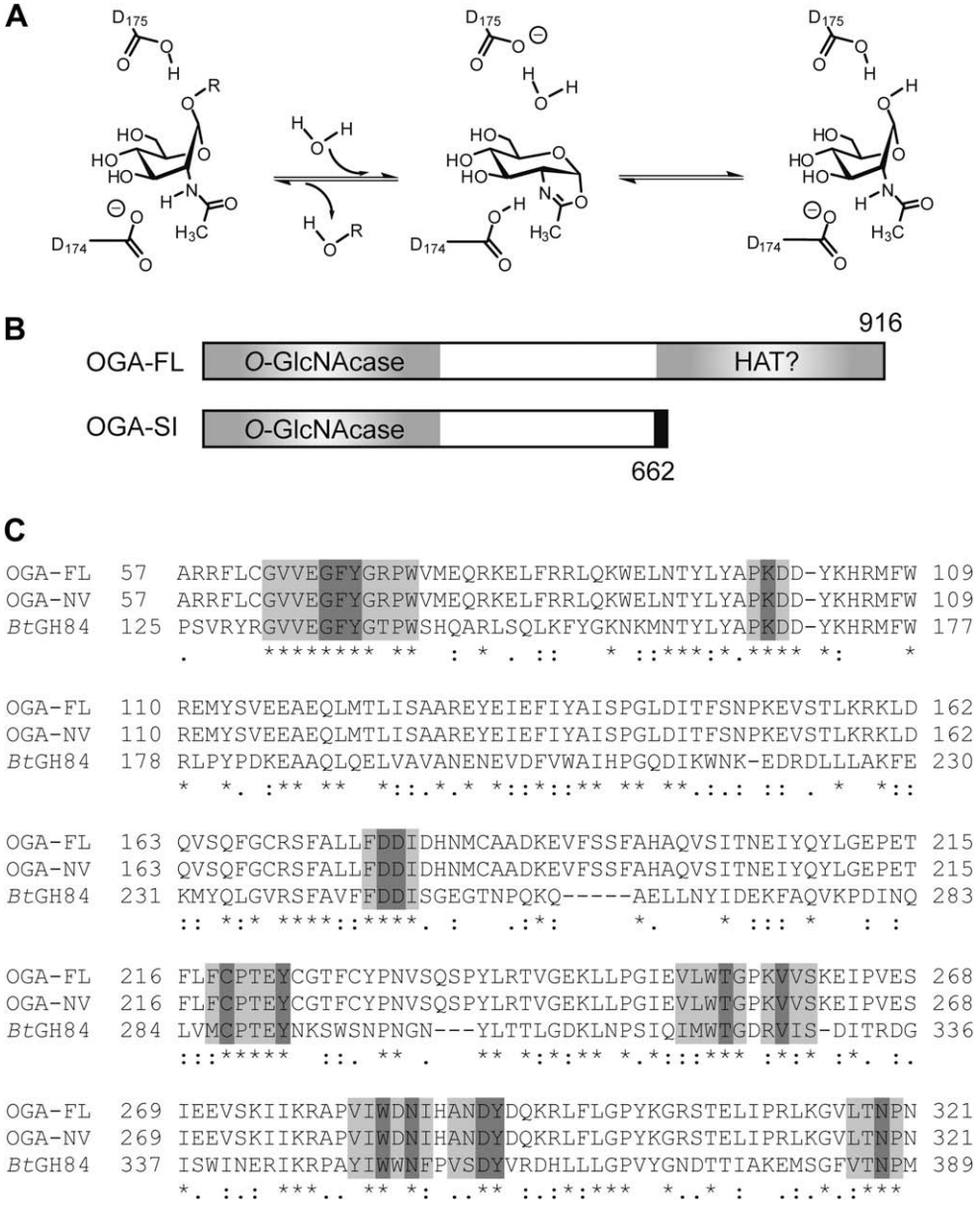

Figure 1. The catalytic domain responsible for *O*-GlcNAcase activity is present in both the nuclear variant (OGA-NV) and the full-length form of OGA (OGA-FL). (A) The proposed catalytic mechanism of OGA involves a two-step double displacement mechanism involving the transient formation of an oxazoline intermediate. Asp174 likely acts in the first step as a general base, orienting and enhancing the nucleophilicity of the 2-acetamido group toward the anomeric center. Departure of the leaving group is aided by Asp175, which acts as a general acid catalyst. The second step of the reaction is the near microscopic reverse of the first step; water acts as a nucleophile to attack the anomeric center and open the oxazoline ring. (B) Schematic showing the architecture of OGA-NV. OGA-NV lacks a putative histone acetyl transferase (HAT) C-terminal domain. In addition, the OGA-NV contains an additional 15 amino acids (filled black box) encoded by part of intron 10, which is not spliced out in this isoform. (C) Sequence alignment of the GH84 catalytic domain of OGA-FL (meningioma expressed antigen 5, NP_036347), OGA-NV (meningioma expressed antigen 5, NP_036347), and a bacterial homologue of *O*-GlcNAcase from *B. thetaiotamicron* (*Bt*GH84) (hyaluronoglucosaminidase precursor, NP_813306). Highlighted in light gray are residues that are within 8 Å of NAG-thiazoline in a structure with *Bt*GH84[22] (PDB 2CHO) and residues highlighted in darker gray are those that make contacts (<4 Å) with NAG-thiazoline. Notably, the active site residues are completely conserved between the three enzymes. Sequence alignment was performed using ClustalW.[33]

reported to have histone acetyl transferase (HAT) activity,[18] although more recent efforts have failed to support these findings.[19] Cell fractionation studies provided evidence that OGA-NV resides in the nucleus,[14] whereas OGA-FL is predominantly cytosolic.[20] Unexpectedly, OGA-NV was reported to have no detectable glycoside hydrolase activity toward the chromogenic substrate *p*-nitrophenyl 2-acetamido-2-deoxy-β-D-glucopyranoside (*p*NP-GlcNAc)[17] but could be assayed with a more sensitive fluorogenic substrate.[17] Furthermore, OGA-NV was shown to be active on *O*-GlcNAc-modified proteins, albeit at a diminished rate compared to OGA-FL.[17] More recently it was reported that OGA-NV was not inhibited by two inhibitors of OGA-FL; *O*-(2-acetamido-2-deoxy-D-glycopyranosylidene)amino-*N*-phenylcarbamate (PUG-NAc, Fig. 2a) and 1,2-dideoxy-2′-methyl-α-D-glucopyranoso-[2,1-*d*]-Δ2′-thiazoline (NAG-thiazoline, Fig. 2b).[21] While these two inhibitors have nanomolar potencies against OGA-FL,[7] it was reported that OGA-NV was only inhibited 50% when they were used at a concentration of 0.5 mM.[21] Based on these studies it was proposed that the active site of OGA-NV may differ from that of OGA-FL.[21] These discrepancies between OGA-FL and OGA-NV in activity and susceptibility to inhibition are important in the context of defining the functional roles of these two isoforms in biological systems. Because these isoforms of OGA may have different, or compensatory, functional roles, the inhibition of only one of them

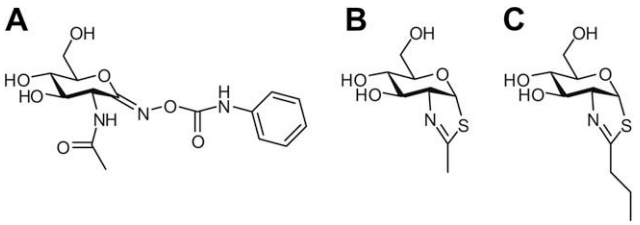

Figure 2. Structures of several *O*-GlcNAcase inhibitors tested in this study. (A) PUGNAc, (B) NAG-thiazoline, (C) NButGT. While PUGNAc and NAG-thiazoline also inhibit other functionally related enzymes, NButGT is highly selective for *O*-GlcNAcase.

could therefore lead to different effects then when inhibiting both these isoforms.

Based on structural studies of a bacterial homologue of OGA from *Bacteroides thetaiotamicron* (*Bt*GH84)[22] and the common conservation of all the active site residues of OGA-FL, OGA-NV, *Bt*GH84 (Fig. 1c) we were surprised by the apparent 10,000-fold decrease in affinity toward these inhibitors reported previously, as well as the decreased catalytic efficiency of OGA-NV relative to OGA-FL. To address this apparent discrepancy, we therefore cloned OGA-NV, characterized the enzymatic properties of this enzyme using various assays, and determined its affinity to several known OGA-FL inhibitors.

2. Results and discussion

2.1. Initial characterization of MBP-tagged OGA-NV

Previously, reports have suggested that OGA-NV has no apparent activity toward *p*NP-GlcNAc.[17] Using purified recombinant MBP-tagged OGA-NV we found, with careful measurement and using concentrated enzyme, detectable activity that could be readily described by Michaelis–Menten kinetics (Fig. 3). This OGA-NV construct bearing a maltose-binding protein affinity tag showed comparable kinetics to the more poorly expressing OGA-NV construct bearing a His_6-tag (data not shown); indicating that the presence of the MBP on OGA-NV does not significantly impair catalysis. Although the K_M was only increased twofold (OGA-NV K_M = 0.32 ± 0.05 mM; OGA-FL K_M = 0.16 ± 0.02 mM), V_{max} was decreased 200-fold for OGA-NV (OGA-NV V_{max} = 0.007 ± .001 μmoles min^{-1} mg^{-1}) as compared to OGA-FL (OGA-FL V_{max} = 1.3 ± 0.1 μmoles min^{-1} mg^{-1}). Therefore, the catalytic efficiency of OGA-NV is approximately 400-fold lower than OGA-FL when using *p*NP-GlcNAc as a substrate. Although we were able to assay the enzyme using this substrate, an extremely large concentration of enzyme (>5 μM) was required to obtain significant rates. Such high concentrations of enzyme are undesirable when testing potent inhibitors as they prevent accurate measurement of K_I values of less than fivefold the enzyme concentration. We therefore resorted to a continuous fluorescence-based assay. Using 4-MU-GlcNAc as the substrate we were able to use much less enzyme (100 nM) in our reactions. Michaelis–Menten parameters were obtained using this substrate and a similar difference (400-fold) in catalytic efficiencies between OGA-FL and OGA-NV was obtained (data not shown). It should also be noted that a construct of *O*-GlcNAcase consisting of residues 1–662 but lacking the extra 15 amino acids from intron 10 had a similar decrease in catalytic efficiency, suggesting that these amino acids do not alter the catalytic properties of OGA-NV (data not shown). These data support previous observations that the activity of OGA-NV is significantly impaired.[14,17]

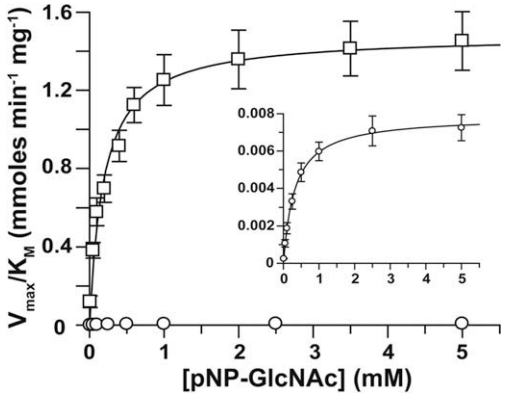

Figure 3. Michaelis–Menten kinetics for the two isoforms of OGA; OGA-FL and OGA-NV. Inset is zoomed in view showing the activity of OGA-NV. The kinetic parameters for OGA-FL are: V_{max} = 1.3 μmol min^{-1} mg^{-1}; K_M = 0.16 mM, whereas OGA-NV has the following kinetic parameters: V_{max} = 0.007 μmol min^{-1} mg^{-1}; K_M = 0.32 mM. Therefore, the catalytic efficiency (V_{max}/K_M) of OGA-NV is approximately 400-fold lower than that of OGA-FL when using *p*NP-GlcNAc as the substrate. Data are the average of triplicate rate measurements and error bars represent standard deviations.

2.2. Further enzymatic characterization of OGA-NV

To further characterize OGA-NV we next analyzed its pH-rate profile. This rate profile was very similar to that observed previously for OGA-FL[9] with an activity maximum of pH 6.5 and a broad

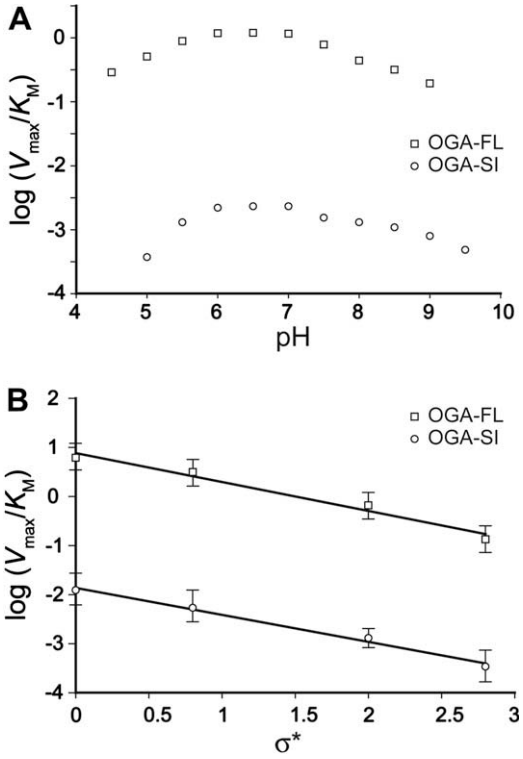

Figure 4. Further enzymatic characterization of OGA-NV. (A) The pH-rate profiles of OGA-FL and OGA-NV reveal a similar shape using 4-MU-GlcNAc as the substrate. (B) OGA-FL and OGA-NV were tested using a series of four different 4-MU-GlcN-Acyl substrates that have various degrees of fluorination (0, 1, 2, or 3) on the methyl group of the 2-acetamido group. The resulting logarithm of the second order rate constants (V_{max}/K_M) was plotted as function of the Taft electronic parameter σ^*. The similar slopes (ρ) of these Taft plots imply a similar degree of acetamido participation, suggesting that the two enzymes use broadly similar transition states. Data points in panel A represent the average of two measurements. Error bars in panel B represent the error of the data fit used to obtain the V_{max}/K_M values.

bell-shape (Fig. 4a). The similarity in the shape of the pH-rate profile suggests that the molecular architecture of the *O*-GlcNAcase active site is not significantly disrupted in the nuclear variant OGA-NV. We also carried out a linear free energy analysis using substrates with different levels of fluorination on the 2-acetamido group of 4-MU-GlcNAc. As previously described,[7] this Taft analysis correlates the effect of an electronic parameter for the corresponding 2-acetamido group (σ^*) to the logarithm of the second order rate constant ($\log(k_{cat}/K_M)$).

Glycosidases that use substrate-assisted catalysis display negative slopes in such Taft analyses due to the involvement of this moiety as a nucleophile during catalysis to form a transient oxazoline intermediate.[7,23] Accordingly, the second order rate constant for the hydrolysis of a series of fluorinated 4-MU-GlcNAc substrates was measured using OGA-NV and plotted against the Taft electronic parameter σ^* to give a negative slope (ρ) of -0.51 ± 0.07 (Fig. 4b). We previously reported a ρ-value of -0.42 for OGA-FL, however, a pH of 6.5 was used in those assays.[7] The current studies with OGA-NV were carried out at a more physiologically relevant pH of 7.4 and we therefore repeated the study at this pH with OGA-FL, which gave us a ρ-value of -0.59 ± 0.06 (Fig 3b). Because these ρ-values report on the aspects of the structure of the transition state, particularly the involvement of the acetamido group as a nucleophile, the statistically indistinguishable ρ-values for the two isoforms strongly suggest that they carry out catalysis via broadly similar transition states.

Therefore, despite OGA-NV and OGA-FL very likely having identical active site structures and using similar transition states, there is still a 400-fold difference in catalytic efficiency between the two isoforms. It is difficult to ascertain the basis for this difference, however, we cannot rule out the possibly that the C-terminal domain plays a role in facilitating catalysis directly, enzyme stability, or enzyme dynamics. This view seems consistent with a recent report demonstrating that the C-terminal domain appears to rescue the catalytic activity of the N-terminal domain when added in vitro to enzyme assays.[19] Given these observations we felt it would be worthwhile examining whether some of the established and more widely used inhibitors of OGA-FL were potent against OGA-NV, which would be expected based on the above-mentioned results, or whether some of these were genuinely poor inhibitors of OGA-NV as previously reported.[21]

2.3. Inhibition of OGA-NV

Two classes of inhibitors of OGA-FL have been fairly well characterized and are used more widely. The first described inhibitor of OGA-FL was PUGNAc[6] (Fig. 2a) and it has been widely used as a means of elevating *O*-GlcNAc levels in a cellular context.[24] Unfortunately, PUGNAc lacks selectivity for OGA over the functionally related lysosomal β-hexosaminidases[17] and some of the phenotypes associated with using PUGNAc may not stem from elevation of *O*-GlcNAc levels.[7,25] More recently, we found[7] that NAG-thiazoline (Fig. 2b)[26] is a potent inhibitor of OGA. Like PUGNAc, NAG-thiazoline has a nanomolar affinity toward OGA-FL but it is equally potent against the lysosomal β-hexosaminidases.[7] To circumvent this problematic lack of selectivity for OGA, we generated a series of selective inhibitors related to NAG-thiazoline and we were able to realize up to 35,000-fold selectivity for OGA-FL.[7,27] One such selective inhibitor, NButGT (Fig. 2c), is proving to be a useful tool for studying the biological role of the *O*-GlcNAc modification.[25]

Given the effectiveness of these particular inhibitors in modulating OGA-FL activity in vitro,[6,7] in cell culture,[7,24] tissues studied ex vivo,[28] and in vivo[27,29] we felt it is important to clarify their targets. This is particularly important as a previous study reported that PUGNAc and NAG-thiazoline are poor inhibitors of OGA-NV,[21] a finding that seems difficult to reconcile with the high level of conservation of the GH84 catalytic domain (and complete conservation of the active site) coupled to the similar trends in the pH-rate profiles and Taft analyses. Indeed, these data argue that the two isoforms carry out catalysis via similar transition states and therefore, given that NAG-thiazoline has been shown to act as a transition state analogue,[30] it was surprising to us that it was reportedly ineffective against OGA-NV. Such an inability to inhibit OGA-NV could complicate the interpretation of data obtained using these inhibitors in cell culture because OGA-NV and OGA-FL may have different, or compensatory, physiological roles.

We therefore tested PUGNAc and NAG-thiazoline as inhibitors of OGA-NV and found that, at a concentration of 500 nM, they resulted in approximately 50% inhibition when using a substrate concentration of 0.25 mM. Due to the requirement for substantial amounts of enzyme (100 nM) in our fluorogenic assay, we were however unable to determine an accurate K_I value, although these data suggest that these inhibitors are similarly potent against OGA-NV as OGA-FL. To evaluate this issue more carefully we therefore turned our attention to the selective inhibitor NButGT as it is slightly less potent (K_I = 600 nM). We find that NButGT is a good inhibitor of OGA-NV and it shows a clear pattern of competitive inhibition (Fig. 5a and b). The K_I value (1.5 ± 0.3 μM) (Fig. 5c) we determine is only approximately threefold higher than that observed for OGA-FL (K_I = 600 nM for OGA-FL) at the same pH.[7] We also tested the product of the reaction (GlcNAc) as an inhibitor of OGA-NV and found a K_I value of 3.6 ± 0.5 mM (Fig. 5d–f), which is again approximately threefold higher than that reported previously for OGA-FL (K_I = 1.5 mM for OGA-FL).[7] This slightly weaker binding may be consistent with the twofold increased in K_M exhibited by OGA-NV. The discrepancy between our results and those obtained previously by others[21] could stem from a number of complicating factors, perhaps most notably is that crude *Escherichia coli* extracts containing overexpressed OGA-NV were used in those studies rather than purified protein that we use here. As a consequence, the concentration of OGA-NV in assays from that earlier study may have been high and precluded accurate determination of K_I values. Further complicating the use of bacterial lysates in these inhibition assays is that *E. coli* has a functionally related β-*N*-acetylglucosaminidase known as NagZ, which will readily cleave β-O-linked glucosaminide substrates.[31] The presence of NagZ may give rise to an overestimate of *O*-GlcNAcase activity in these assays.[17,21]

3. Conclusions

In summary, careful analyses reveal that OGA-NV has kinetic properties similar to OGA-FL except that the catalytic efficiency of OGA-NV is 400-fold lower than that found for OGA-FL. Furthermore, OGA-NV carries out catalysis through transition states that resemble those used by OGA-FL and both isoforms use the same catalytic mechanism. Consistent with this view, OGA-NV is also powerfully inhibited by the same inhibitors that inhibit OGA-FL indicating that NButGT, and very likely other inhibitors selective for human OGA over the lysosomal hexosaminidases, will act to block the activities of both these isoforms. These findings indicate that inhibition of OGA in cell culture and in vivo using these inhibitors likely does not permit functional compensation of OGA-FL inhibition by continued action of OGA-NV.

4. Experimental

4.1. General

All salts and buffers were obtained from Bioshop. Substrates were obtained from Sigma. Activity assays with pNP-GlcNAc were

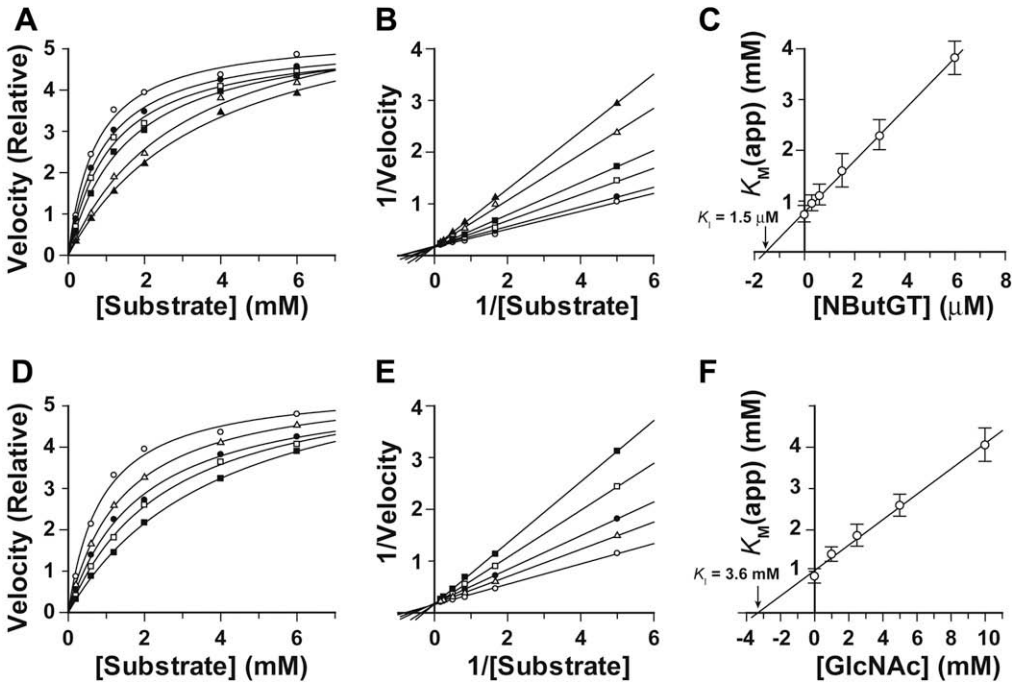

Figure 5. NButGT is a potent inhibitor of OGA-NV. Inhibition studies of OGA-NV using NButGT (A–C) and GlcNAc (D–F) as inhibitors. Michaelis–Menten (A, D) and Lineweaver–Burk plots (B, E) reveal a clear pattern of competitive inhibition. Replots of the apparent K_M versus inhibitor concentration (C, F) reveal K_I values of 1.5 μM and 3.6 mM for NButGT and GlcNAc, respectively. Data points in panels A, B, D, and E represent the average of triplicate measurements. Error bars are not shown for purposes of clarity. Error bars in panels C and F represent the errors in $K_{M(apparent)}$ values obtained from fitting of full Michaelis–Menten kinetic data (shown in panels A and D) at each inhibitor concentration.

monitored using a UV–vis spectrophotometer (Cary 3E UV–vis) and assays with 4-methylumbelliferyl 2-acetamido-2-deoxy-β-D-glucopyranoside (4-MU-GlcNAc) were monitored using a fluorimeter (Varian CARY Eclipse). The preparation of PUGNAc,[32] NAG-thiazoline,[26] and 1,2-dideoxy-2′-propyl-α-D-glucopyranoso-[2,1-d]-Δ2′-thiazoline (NButGT)[7] has been described elsewhere. 4-MU-GlcNAc substrates bearing varying levels of fluorination on the 2-acetamido group were prepared as described previously.[7]

4.2. Cloning

OGA-NV contains 15 amino acids that are encoded by the start of intron 10. Because these nucleotides are not available within a cDNA clone of OGA, they were incorporated within primers using two successive rounds of PCR. For the first round of PCR, the forward and reverse primers were: 5′-GCCGCCCATATGGTGCAGAAGG AGAGTCAAGCG-3′ and 5′-GCCGCCCTCGAGGAAGAGATTATTCCTG GTGCACCTACCTAACCACTGTACAAAA-GAC-3′, respectively. This PCR product was used in a second round of PCR using the same forward primer but with the reverse primer: 5′GCCGCCCTCGAGTT AAAGGGACAATATAT-TTGAGGAGAAGAGATTATTCCTGGTGCACC-3′. This elongated PCR product was ligated into pET28a (Novogen) using the NdeI and XhoI restriction sites to generate a His_6-tagged fusion protein, however, yields of the resulting recombinant protein were very low (data not shown). We therefore subsequently subcloned OGA-NV into the pMal-C2X vector using the SalI and BamHI restriction sites to produce a construct encoding a protein bearing an N-terminally fused maltose binding protein (MBP).

4.3. Expression and purification

The pMal-C2X vector (New England Biolabs) containing OGA-NV was transformed into tuner BL21 ΔDE3 cells (Novagen) for expression. Cells were induced with 0.5 mM IPTG when the OD_{600} of the culture reached 0.8. After 3 h of induction at room temperature, cells were pelleted by centrifugation (5000 rpm, 10 min) and resuspended in PBS containing 1 mM EDTA. Cells were lysed using a combination of incubation with 1 mg/ml lysozyme for 30 min at room temperature as well as sonication (6 cycles, 20 s, 50% duty). The cell debris was pelleted by centrifugation (15,000 rpm, 1 h) and the supernatant was loaded onto a 5 ml Dextrin Sepharose column (GE Healthcare), washed with 100 ml of PBS containing 1 mM EDTA, and eluted in 25 ml of PBS containing 20 mM maltose. The fractions containing purified OGA-NV were concentrated to a volume of 2 ml and loaded onto a gel filtration chromatography on a Sephacryl S-300 size-exclusion column (GE Healthcare). Fractions containing OGA-NV were identified by SDS–PAGE as well as by fluorescence-activity assays (see below), pooled, and then dialyzed against PBS. Purification of OGA-FL has been described previously.[8]

4.4. Kinetics

Initial rates of hydrolysis of *p*NP-GlcNAc and 4-MU-GlcNAc were measured as described previously.[8,27] The pH-rate profile was carried out in buffer containing 50 mM citric acid, 50 mM sodium phosphate, 50 mM CHES, and 100 mM sodium chloride adjusted to the appropriate pH. The extinction coefficient at each respective pH was determined using the Beer–Lambert law by measuring the absorbance of several concentrations of *p*-nitrophenolate in the appropriate buffer. To quantitate turnover of 4-MU-GlcNAc a standard curve was constructed bracketing the range of fluorescence measurements made during enzyme activity assays. The Taft analysis was carried out by continuous monitoring of the liberated 4-methylumberlliferone product using PBS (pH 7.4) as a buffer.

Acknowledgments

This research was supported by grants from the Canadian Institutes for Health Research (CIHR) and the Natural Sciences and Engineering Research Council of Canada (NSERC) to D.J.V. is a scholar of the Michael Smith Foundation for Health Research (MSFHR) and M.S.M is a recipient of a senior graduate fellowship from the MSFHR and NSERC. D.J.V. is the Canada Research Chair in Chemical Glycobiology. We thank Andy Bennet for use of the UV/vis spectrophotometer and fluorimeter. Keith Stubbs is thanked for providing the PUGNAc used in these studies.

References

1. Hart, G. W.; Housley, M. P.; Slawson, C. *Nature* **2007**, *446*, 1017–1022.
2. Torres, C. R.; Hart, G. W. *J. Biol. Chem.* **1984**, *259*, 3308–3317.
3. Roquemore, E. P.; Chevrier, M. R.; Cotter, R. J.; Hart, G. W. *Biochemistry* **1996**, *35*, 3578–3586.
4. Chou, C. F.; Smith, A. J.; Omary, M. B. *J. Biol. Chem.* **1992**, *267*, 3901–3906.
5. Haltiwanger, R. S.; Holt, G. D.; Hart, G. W. *J. Biol. Chem.* **1990**, *265*, 2563–2568.
6. Dong, D. L.; Hart, G. W. *J. Biol. Chem.* **1994**, *269*, 19321–19330.
7. Macauley, M. S.; Whitworth, G. E.; Debowski, A. W.; Chin, D.; Vocadlo, D. J. *J. Biol. Chem.* **2005**, *280*, 25313–25322.
8. Macauley, M. S.; Stubbs, K. A.; Vocadlo, D. J. *J. Am. Chem. Soc.* **2005**, *127*, 17202–17203.
9. Cetinbas, N.; Macauley, M. S.; Stubbs, K. A.; Drapala, R.; Vocadlo, D. J. *Biochemistry* **2006**, *45*, 3835–3844.
10. Cheung, W. D.; Hart, G. W. *J. Biol. Chem.* **2008**, *283*, 13009–13020.
11. Taylor, R.; Chambers, J.; Geisler, T.; McClain, D. *Diabetes* **2008**, *57*, A705.
12. Kreppel, L. K.; Blomberg, M. A.; Hart, G. W. *J. Biol. Chem.* **1997**, *272*, 9308–9315.
13. Hanover, J. A.; Yu, S.; Lubas, W. B.; Shin, S. H.; Ragano-Caracciola, M.; Kochran, J.; Love, D. C. *Arch. Biochem. Biophys.* **2003**, *409*, 287–297.
14. Comtesse, N.; Maldener, E.; Meese, E. *Biochem. Biophys. Res. Commun.* **2001**, *283*, 634–640.
15. Love, D. C.; Kochan, J.; Cathey, R. L.; Shin, S. H.; Hanover, J. A. *J. Cell. Sci.* **2003**, *116*, 647–654.
16. Lazarus, B. D.; Love, D. C.; Hanover, J. A. *Glycobiology* **2006**, *16*, 415–421.
17. Kim, E. J.; Kang, D. O.; Love, D. C.; Hanover, J. A. *Carbohydr. Res.* **2006**, *341*, 971–982.
18. Toleman, C.; Paterson, A. J.; Whisenhunt, T. R.; Kudlow, J. E. *J. Biol. Chem.* **2004**, *279*, 53665–53673.
19. Butkinaree, C.; Cheung, W. D.; Park, S.; Park, K.; Barber, M.; Hart, G. W. *J. Biol. Chem.* **2008**, *283*, 23557–23566.
20. Gao, Y.; Wells, L.; Comer, F. I.; Parker, G. J.; Hart, G. W. *J. Biol. Chem.* **2001**, *276*, 9838–9845.
21. Kim, E. J.; Amorelli, B.; Abdo, M.; Thomas, C. J.; Love, D. C.; Knapp, S.; Hanover, J. A. *J. Am. Chem. Soc.* **2007**, *129*, 14854–14855.
22. Dennis, R. J.; Taylor, E. J.; Macauley, M. S.; Stubbs, K. A.; Turkenburg, J. P.; Hart, S. J.; Black, G. N.; Vocadlo, D. J.; Davies, G. J. *Nat. Struct. Mol. Biol.* **2006**, *13*, 365–371.
23. Vocadlo, D. J.; Withers, S. G. *Biochemistry* **2005**, *44*, 12809–12818.
24. Haltiwanger, R. S.; Grove, K.; Philipsberg, G. A. *J. Biol. Chem.* **1998**, *273*, 3611–3617.
25. Macauley, M. S.; Bubb, A. K.; Martinez-Fleites, C.; Davies, G. J.; Vocadlo, D. J. *J. Biol. Chem.* **2008**, *283*, 34687–34695.
26. Knapp, S.; Vocadlo, D.; Gao, Z. N.; Kirk, B.; Lou, J. P.; Withers, S. G. *J. Am. Chem. Soc.* **1996**, *118*, 6804–6805.
27. Yuzwa, S. A.; Macauley, M. S.; Heinonen, J. E.; Shan, X.; Dennis, R. J.; He, Y.; Whitworth, G. E.; Stubbs, K. A.; McEachern, E. J.; Davies, G. J.; Vocadlo, D. J. *Nat. Chem. Biol.* **2008**, *4*, 483–490.
28. Arias, E. B.; Kim, J.; Cartee, G. D. *Diabetes* **2004**, *53*, 921–930.
29. Zou, L.; Yang, S.; Hu, S.; Chaudry, I. H.; Marchase, R. B.; Chatham, J. C. *Shock* **2007**, *27*, 402–408.
30. Whitworth, G. E.; Macauley, M. S.; Stubbs, K. A.; Dennis, R. J.; Taylor, E. J.; Davies, G. J.; Greig, I. R.; Vocadlo, D. J. *J. Am. Chem. Soc.* **2007**, *129*, 635–644.
31. Stubbs, K. A.; Balcewich, M.; Mark, B. L.; Vocadlo, D. J. *J. Biol. Chem.* **2007**, *282*, 21382–21391.
32. Stubbs, K. A.; Zhang, N.; Vocadlo, D. J. *Org. Biomol. Chem.* **2006**, *4*, 839–845.
33. Larkin, M. A.; Blackshields, G.; Brown, N. P.; Chenna, R.; McGettigan, P. A.; McWilliam, H.; Valentin, F.; Wallace, I. M.; Wilm, A.; Lopez, R.; Thompson, J. D.; Gibson, T. J.; Higgins, D. G. *Bioinformatics* **2007**, *23*, 2947–2948.